COLLECTION EFFECTS ON CLOSE PARALLEL BARE TETHERS

Juan R. Sanmartín
ETSI Aeronáuticos, Universidad Politécnica de Madrid, 28040 Madrid, Spain

R.D. Estes
Smithsonian Astrophysical Observatory, 60 Garden St., Cambridge, MA 02138

Abstract

We review previously published results, and present new results, on the way current to a cylindrical probe drops below the orbital-motion-limited (OML) value for probe cross-sections too large or concave. Results on size and shape effects arise from unrelated behavior in the near and far potential field, and apply to a general cross-section, which can be characterised by radius R_{eq} and perimeter p_{eq} of equivalent circles. These results are used to discuss collection interference among two or more parallel bare tethers when brought from far away to contact.

Introduction

At positive bias, the electron current I to a cylindrical probe in an unmagnetized plasma with electron distribution function isotropic at infinity and no trapped-orbit population, has an upper bound,

$$I \le I_{OML} \text{ (OML current).}$$

The probe reaches this bound if its cross-section is both small and convex enough. At the very high bias of interest for bare tethers, the OML current is

$$I_{OML} \approx (p/\pi)\, LeN_\infty \sqrt{2e\Phi_p/m_e} \propto p. \qquad (1)$$

Here, L, Φ_p and p are probe length, bias, and perimeter of its cross-section, and N_∞ is the unperturbed electron density. We had discussed elsewhere magnetic and trapped-orbit effects[1] and the anisotropy arising in the bare-tether case from its orbital velocity.[2, 3]

As we shall see, current fails to reach the OML value if the cross-section is either large or nonconvex, with either type of failure relating to a quite different feature in the potential field. We consider separately the effects of size and shape. We then use results in a simple discussion of interference effects among two or more parallel bare tethers, showing how total current decreases as distances among them decrease.

Size Effect

Probe with circular cross-section

The symmetry of this basic problem allows determining a complete solution for potential field and current. As shown in Ref.1, one finds

$$I = I_{OML} \quad for \quad p/2\pi = R < R_{max}, \qquad (2)$$

$$R_{max} = \lambda_{De} \times function\,[e\Phi_p/kT_e,\ T_i/T_e]. \qquad (2')$$

Here λ_{De} is the electron Debye length; typically, the ratio R_{max}/λ_{De} is about unity for parametric values of interest (Fig.1),

$$T_i/T_e \sim 1, \quad e\Phi_p/kT_e \sim 10^3. \qquad (3)$$

When R increases beyond R_{max} (or λ_{De} decreases with growing density N_∞, at fixed R), the current drops below the OML value, as a size effect related to the behavior of the potential profile far from the probe; for $R > R_{max}$, collection is affected by potential barriers in a distant region between certain radii r_0 and r_1 (Figs.2, 3),

$$r_0 > r_1 \sim R\sqrt{e\Phi_P/kT_i} >> R, \qquad (4)$$

where the profile gets steeper. Then, trajectories that would hit the probe within some range of glancing angles are unpopulated: the probe being attractive, they would had come, not from the faraway, background plasma, but from other points on the (non-emissive) probe, after having turned back inside that region (Fig.4).

Preliminary, approximate (asymptotic) results for the ratio I/I_{OML} beyond R_{max} were advanced in Ref.3. We have now determined complete results (a sample shown in Fig.5), that take the form

$$I/I_{OML} = function\,[R/\lambda_{De},\ e\Phi_p/kT_e,\ T_i/T_e]. \qquad (5)$$

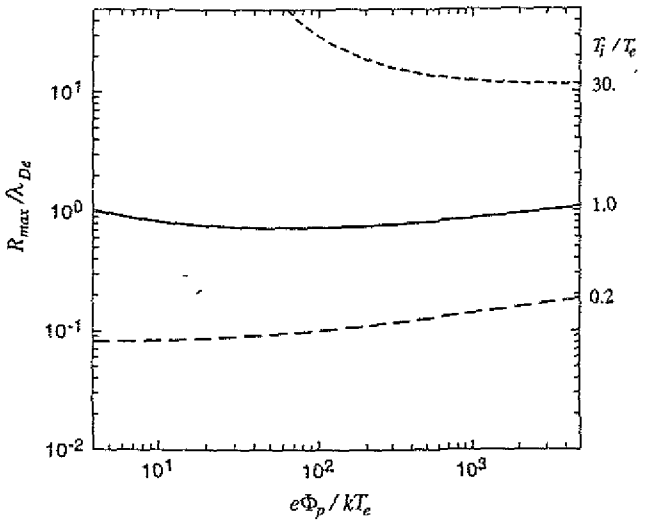

Fig.1. R_{max}/λ_{De} **versus** $e\Phi_p/kT_e$ **and** T_i/T_e.

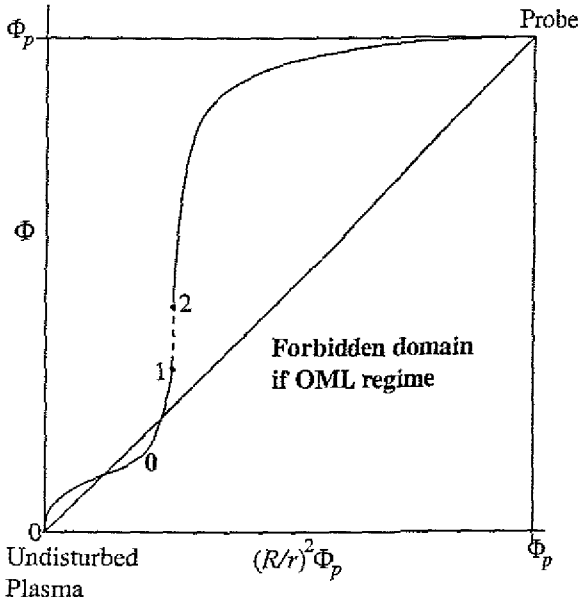

Fig.2. Potential profile for $R_{max} < R$ **. As** R_{max} **drops below** R**, point 0 crosses the diagonal from above. No ions reach above a thin layer at point 2.**

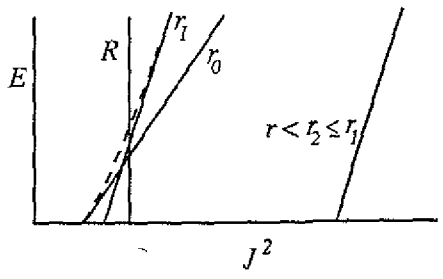

Fig.3. Incoming electrons conserve energy E **and angular momentum** J**. At given** E **and** r**, only orbits with** $J^2 < 2m_e r'^2[E + e\Phi(r')] \equiv J_r'^2(E)$ **for all** $r' > r$ **are populated. Straight lines in the** r**-family** $J^2 = J_r^2(E)$ **get steeper as** r **decreases, but** $J_r^2(0)$ **has a minimum at** r_0**, with** $r_1 < r < r_0$ **lines determining an envelope that crosses the** R**-line for** $R_{max} < R$.

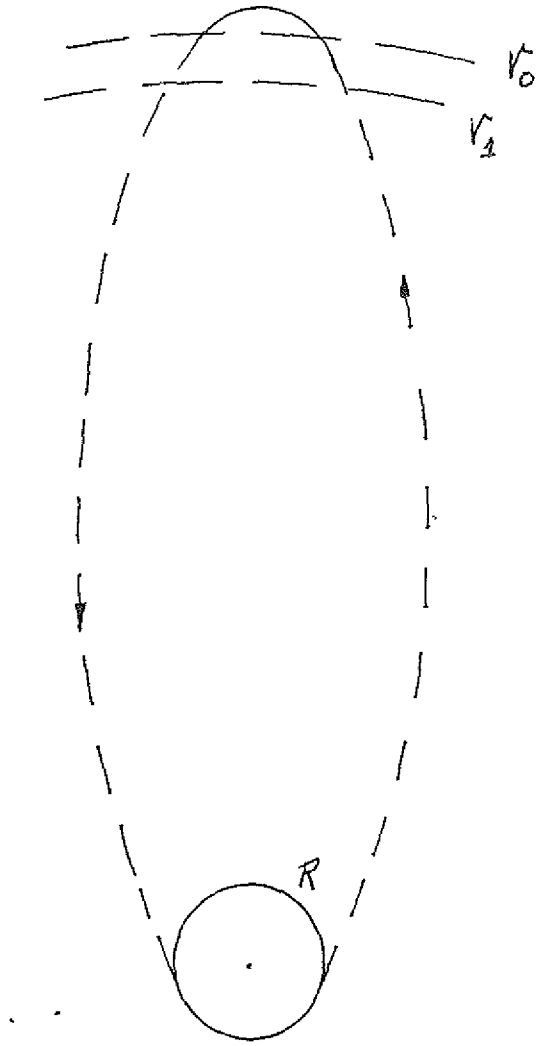

Fig.4. For $R_{max} < R$**, trajectories leaving the probe (backward in time) at a range of glancing angles return to the probe, rather than reaching the background plasma.**

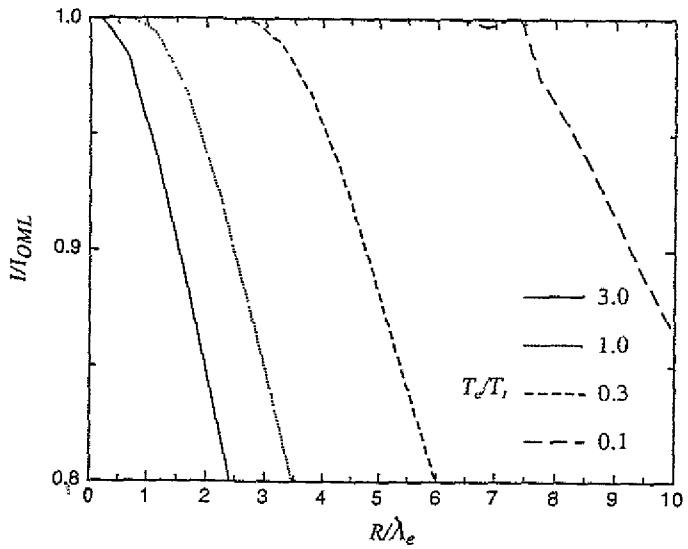

Fig.5. Current ratio I/I_{OML} **versus** R/λ_{De} **and** T_i/T_e**, for** $e\Phi_P/kT_e = 300$.

We note here two additional points of interest. First, because of the high bias, the Laplace equation applies within some probe vicinity where the space charge has negligible effects,

$$\Phi \approx \Phi_P [1 - \alpha \ln (r/R)], \qquad (6)$$

$$\alpha \sim 1/\ln (r_1/R) \quad \text{(moderately small)}. \qquad (7)$$

With all other parameters fixed, α increases weakly with R. At $r = 2R$, say, Eqs.(4), (6) and (7) with $e\Phi_P/kT_e \sim 10^3$ give $\sqrt{\Phi(r)}/\Phi_P \approx 0.9$.

Next, note that we have

$$I_{OML} \propto R\sqrt{\Phi_P} \equiv \sqrt{r^2\Phi(r)} \text{ at } r = R. \qquad (8)$$

If we were to compute the current using $\sqrt{r^2\Phi(r)}$ at $r = 2R$ (rather than at $r = R$) we would overestimate it by a factor near 2. This relates to the fact that all trajectories reaching $r = R$ from infinity are obviously hitting the probe, whereas trajectories reaching $r = 2R$ within some range of glancing angles will miss it.

Probes with elliptical cross-sections

A value $w = w_P$ in elliptical coordinates v, w,

$$x = a \cos v \cosh w, \qquad y = a \sin v \sinh w$$

$$(0 < v < 2\pi, \qquad 0 < w < \infty),$$

serves to describe an elliptical cross-section of semiaxes a_e, b_e,

$$a_e = a \cosh w_P, \qquad b_e/a_e = \tanh w_P.$$

Because of the high bias, the Laplace equation is again valid within some probe vicinity that reaches where w ellipses are near-circles,

$$w \approx \ln (2r/a) \quad \text{for} \quad w > w^* \text{ (say, 1.5)}. \qquad (9)$$

It may then be argued that $\Phi(v, w)$ is nearly independent of v everywhere, as shown in Ref.1 for the limit case of a vanishingly thin tape ($w_P = 0$).

From the Laplace equation in the probe vicinity we then have

$$d^2\Phi/dw^2 \approx 0 \quad \Rightarrow \quad \Phi \approx \Phi_P [1 - \alpha (w - w_P)].$$

Using (9) and $w_P \equiv \ln [(a_e + b_e)/a]$, we have, near the probe but beyond w^*,

$$\Phi \approx \Phi_P [1 - \alpha \ln (r / R_{eq})],$$

$$R_{eq} \equiv \tfrac{1}{2} (a_e + b_e), \qquad (10)$$

to be compared with Eq.(6). Beyond w^*, the potential behaves as in the case of a circle of radius R_{eq}. Limit ratios $b_e/a_e = 1$ and 0 correspond to circles ($R_{eq} = p/2\pi$) and tapes ($R_{eq} = p/8$) respectively.[1]

Other probe cross-sections

For any family of similarity cross-sections parametrized by size, one can determine certain 'average' half-width R_{eq}, by solving the Laplace equation between the contour of the cross-section and a much larger circle; at intermediate distances, then, the potential takes the form (6) with R_{eq} standing for R. As an example, for a square cross-section we find

$$R_{eq} \approx 0.58 \times \textit{side of the square}, \qquad (11)$$

$$R_{eq} \approx p/6.9. \qquad (11')$$

The OML law keeps valid as regards size as long as R_{eq} remains below R_{max}. Note that shape details are irrelevant to the size effect. The Laplace equation, valid near the probe, filters out to the far field all information on shape, except for the average half-width R_{eq}.

Shape effect

Failure of the OML law due to shape relates to the behavior of the potential field near the probe, ultimaty dependent on the degree of probe convexity. In the case of a tape ($w_P = 0$) we had found[1]

$$I \approx I_{OML} (1 - \gamma\alpha^2) \quad \text{for} \quad R_{eq} \ (= p/8) < R_{max} \qquad (12)$$

with $\gamma(w_P = 0) \sim 0.1$ and α [given by (4) and (7)] logarithmically small, and increasing with R_{eq}. A tape comes out to be not convex enough, but its shape failure is weak; for the bias of interest the current in (12) lies only about 1% below the OML value.

As in the case of Fig.4, for any point on the tape (Fig.6), trajectories that would hit the probe within some (here narrow) range of glancing angles are unpopulated: they would had come from other points on the tape, here, however, remaining always close to it.[4] This is the origin of the current reduction described by (12), which does not relate to size; it holds no matter how small R_{eq} or p. On the other hand, shape is here determinant; as w_P (or b_e/a_e) increases and ellipses evolve from tape to circle, the coefficient $\gamma(w_P)$ in Eq.(12) will vanish at some w_P, the OML current law certainly holding in the limit case of a circle.

We now note that the reduction of current below the OML value for cross-sections that are small can be substantial if they present definitely

concave segments, as in the case of Fig.7, a cross-section made of two adjoining circles. Trajectories that hit a point on a concave segment would be unpopulated over a wide range of incoming angles. The OML law, nonetheless, may still be used to great accuracy if the actual perimeter p in (1) is replaced by the perimeter p_{eq} of the minimum-perimeter convex envelope of the cross-section, made of segments of the actual cross-section and straight segments. For the case of Fig.7, we have

$$p_{eq} = 2(\pi + 2)R, \qquad (13)$$

$$R_{eq} \approx \tfrac{1}{2}(R + 2R) \approx p_{eq} / 6.85. \qquad (13')$$

Note that the value of $\sqrt{\Phi(r)}/\Phi_P$ averaged over the envelope would be very close to unity. Also, conditions for trajectories in the vicinity of the straight (dashed) segments would be similar to conditions in the tape case as far as convexity is concerned. Finally, all trajectories reaching the envelope would certainly hit the probe; note that the argument following Eq.(8) would apply to any convex envelope of larger perimeter. The introduction of the convex envelope of minimum perimeter thus allows accurate use of the OML law for nonconcave cross-sections, and proves helpful in discussing interference effects in collection.

Interference of parallel tethers

The interference of two or more parallel cylindrical probes as regards current collection may be now discussed on the basis of results for the special case of circular cross-sections, as resumed in Eqs.(2-6), when extended to other cross-sections by our introduction of equivalent radius and perimeter, R_{eq} and p_{eq}. The variety of cases show a mixture of shape and size interference effects. Simple results can be obtained for the limit of adjoining probes.

Compare, first, total current to two thin tapes of perimeter p, in two extreme cases, tapes lying far away, and touching each other as in Fig.8a, respectively. We then clearly have

$$I_\infty = 2I_{OML}(p)\,[1 - \gamma\alpha^2(p)],$$

$$I_0 = I_{OML}(2p)\,[1 - \gamma\alpha^2(2p)],$$

subscripts ∞ and 0 standing for infinite and zero distance between tapes. A ratio $I_0/I_\infty < 1$ represents interference effects. Since $I_{OML}(2p) = 2I_{OML}(p)$, interfertence here arises solely from the small γ-terms in Eq.(12) [$\alpha(2p)$ being larger than $\alpha(p)$], and is negligible, $I_0/I_\infty \approx 1$. Note that in writing I_∞ and I_0 above we ignored size effects, Eq.(2), with R_{max} given by (2'), then implying

$$2p/8 = R_{eq}(2p) < R_{max} \qquad \text{or} \qquad p < 4R_{max}.$$

If this condition is not satisfied there will be substantial interference due to size effects, which can be determined with results as in Fig.5.

Consider, next, tapes lying far away, and touching each other as in Fig.8b, respectively. We would then have, ignoring the very small γ - terms and taking $p < 8R_{max}$,

$$I_0 \approx I_{OML}(p), \qquad I_0/I_\infty \approx \tfrac{1}{2}.$$

The decrease from I_∞ to I_0 would start at a distance over twice r_0, or about $5R\sqrt{e\Phi_P/kT_i}$. Note that the orientation in Fig.8b, while worse from the point of view of shape effects, is not affected by size.

Consider finally the case of Fig.8c, where tapes do not touch each other. It follows from (11) that size effects can be ignored if

$$R_{eq} \approx 0.58 \times p/2 < R_{max}.$$

Even then, however, the current here will be less than $I_{OML}(p_{cr})$ with $p_{cr} = 2p$ the perimeter of the minimum-perimeter convex envelope of the "cross-section": For non-adjoining probes such as these, there are orbits crossing between straight (dashed) segments, which will not contribute to the current collected; also, $\sqrt{\Phi(r)}/\Phi_P$ will be sensibly less than unity on the dashed segments. The current drop below $I_{OML}(p_{cr})$ can be determined, nonetheless, by first solving the Laplace equation for the 2-tape arrangement as in the analysis leading to (11), and then following numerically orbits that start inwards at one dashed segment.

Consider now N circular wires in a straight row, with the distance from one to the next either large or vanishing (Fig.9a). We would have limit current values given by

$$I_\infty = \mathrm{N} \times I_{OML}(p) = I_{OML}(\mathrm{N}p)$$

$$I_0 = I_{OML}(p_{cr}), \qquad p_{cr} = 2\pi R + (\mathrm{N} - 1)4R$$

with I_0/I_∞ approaching $2/\pi \approx 0.64$ at large N. Size effects could be ignored as long as

$$R_{eq} \approx (\mathrm{N} + 1)\,R/2 < R_{max}.$$

Similarly, for N^2 wires arranged in a square array, with next-neighbor distance either large or vanishing as in Fig.9b, we would have

$$I_\infty = \mathrm{N}^2 \times I_{OML}(p) = I_{OML}(\mathrm{N}^2 p),$$

$$I_0 = I_{OML}(p_{cr}), \qquad p_{cr} = 2\pi R + (\mathrm{N} - 1)8R,$$

with I_0/I_∞ approaching $4/\pi N$ at large N. It follows from (11) that size effects could be ignored as long as

$$R_{eq} \approx 0.58 \times N \times 2R < R_{max}.$$

Acknowledgments.

The work by J.R.S. was supported by the *Comisión Interministerial de Ciencia y Tecnología* of *Spain* under Grant PB97-0574-C04-1.

References

1 J.R.Sanmartin and R.D.Estes, *The orbital-motion-limited regime of cylindrical Langmuir probes*, Phys.Plasmas **6**, 395 (1998).

2 J.R.Sanmartín and R.D.Estes, *Validity of the Orbital-Motion-Limited Regime of Cylindrical Probes*, NASA/CP-1998-206900, ed. J.K.Harrison (1998), 399.

3 R.D.Estes and J.R.Sanmartín, *New Results on Bare-Tether Current*, Proc. Spacecraft Charging Technology Conference (1998), Hanscom Air Force Base, MA, 2-6 November 1998.

4 J.G.Laframboise and L.W.Parker; *Probe design for orbit-limited current collection*, Phys. Fluids **16**, 629 (1973).

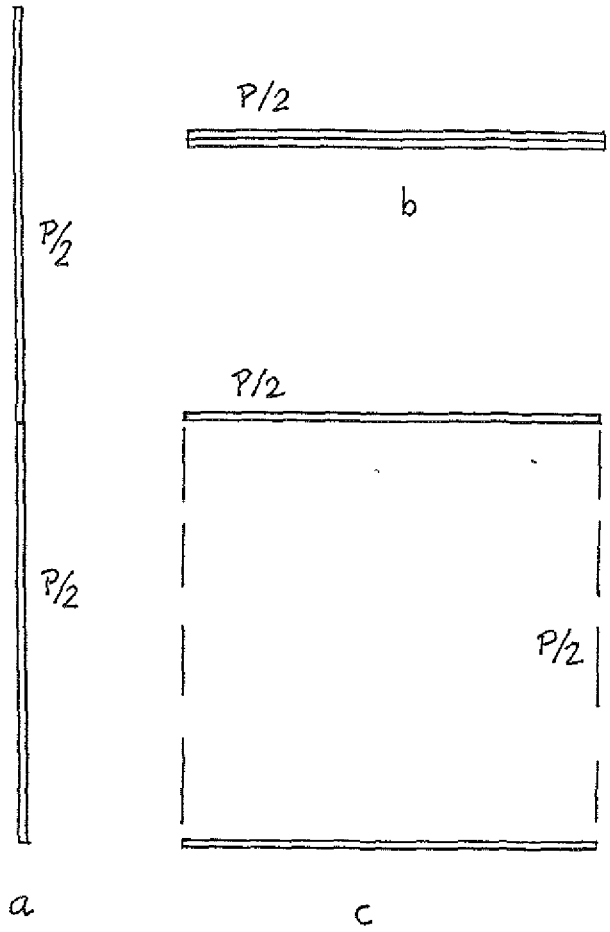

Fig.8a, b, c. Interference between tapes.

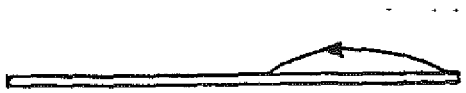

Fig.6. Grazing trajectories connect tape points in the shallow, almost flat potential near the tape.

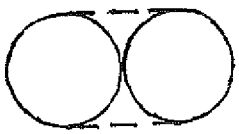

Fig.7. Minimum-perimeter convex envelope (dashed and half-circle segments) for a cross-section made of two adjoining circles.

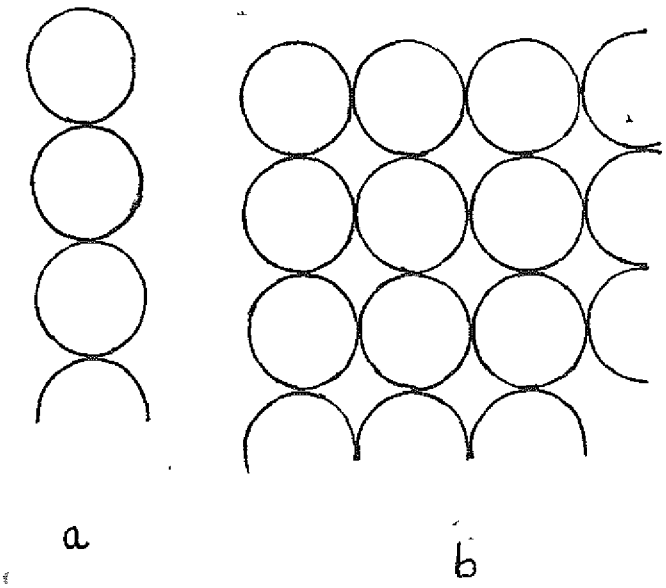

Fig.9. a) Straight row and b) square array of adjoining circles.